Journal of Advances in Mathematics and Computer Science

32(6): 1-14, 2019; Article no.JAMCS.48163
ISSN: 2456-9968
(Past name: British Journal of Mathematics & Computer Science, Past ISSN: 2231-0851)

Cramér-Rao Bound of Direction Finding Using a Uniform Hexagonal Array

Grace Wakarima Ndiritu[1*], Dominic Makaa Kitavi[1] and Cyrus Gitonga Ngari[1]

[1] *Department of Mathematics, Computing and Information Technology, University of Embu, Embu, Kenya.*

Authors' contributions

This work was carried out in collaboration between all authors. Author A designed the study, performed the statistical analysis, wrote the protocol, and wrote the first draft of the manuscript. Author B and Author C managed the analyses of the study. Author C managed the literature searches. All authors read and approved the final manuscript.

Article Information

DOI: 10.9734/JAMCS/2019/v32i630161
Editor(s):
(1) Dr. Amany Mostafa Ibrahim Kawala, Lecturer, Department of Mathematics, Faculty of Science, Helwan University, Egypt.
Reviewers:
(1) Zlatin Zlatev, Trakia University, Bulgaria.
(2) R. Harikumar, Bannari Amman Institute of Technology, India.
(3) Mohamad Awad, National Council for Scientific Research, Lebanon.
Complete Peer review History: http://www.sdiarticle3.com/review-history/48163

Received: 07 February 2019
Accepted: 15 April 2019
Published: 25 June 2019

Original Research Article

Abstract

Direction-of-arrival (DOA) estimation is a key area of sensor array processing which is encountered in many important engineering applications. Although various studies have focused on the uniform hexagonal array for direction finding, there is a scanty use of the uniform hexagonal array in conjunction with Cramér-Rao bound for direction finding estimation. The advantage of Cramér-Rao bound based on the uniform hexagonal array: overcome the problem of unwanted radiation in undesired directions. In this paper, the direction-of-arrival estimation of Cramér-Rao bound based on the uniform hexagonal array was studied. The proposed approach concentrated on deriving the array manifold vector for the uniform hexagonal array and Cramér-Rao bound of the uniform hexagonal array. The Cramér-Rao bound based on the uniform hexagonal array was compared with Cramér-Rao bound based on the uniform circular array. The conclusions are as follows. The Cramér-Rao bound of uniform hexagonal array decreases with an increase in the

**Corresponding author: E-mail: gracendiritu60@gmail.com;*

number of sensors. The comparison between the uniform hexagonal array and uniform circular array shows that the Cramér-Rao bound of the uniform hexagonal array was slightly higher as compared to the Cramér-Rao bound of the uniform circular array. The analytical results are supported by graphical representation.

Keywords: Direction-of-arrival estimation; Array manifold vector; Cramér-Rao bound; Uniform hexagonal array.

2010 Mathematics Subject Classification: 53C25; 83C05; 57N16

1 Introduction

Array signal processing (ASP) is a new algorithm in Digital Signal Processing with many applications. ASP is a fast-growing area in electrical engineering. The area involves analyzing data received on the array of sensors [1]. It is a wide area of research that extends from the simplest one-dimensional to the complex form multi-dimensional. Determining the position of the object or DOA of a signal is one of the expounded estimation tasks.

Direction-of-arrival (DOA) estimation refers to an angle at which a signal impinges on the array of sensors. In the last few decades, accurate determination of DOA from a signal source has received a considerable amount of interest in various fields such as wireless communication, radar, sonar, [2] and military [3]. Military use direction of arrival estimation for anti-jamming and in mobile communication DOA estimation is used to obtain the direction of signal spatial filtering [4].

The idea behind using a sensor array over a single sensor is to improve the accuracy of direction finding. Plane waves are often measured using an array of sensors. A sensor array is composed of elements set out in a particular arrangement. Each sensor converts an electromagnetic wave into a high-potential [5]. Digital sensors arrays have several merits over traditional arrays including enlarged coverage, expanded system capacity, and resistance to two waves superpose to form a resultant wave. They also have the ability to ascertain an incoming signal of direction finding[6]. The hexagonal array is widely used in practice but has obtained less attention in the field of array signal processing [7]. Uniform hexagonal array occurs if the sensors are placed on a single hexagon with uniform spacing. The hexagon is presented in this study since it overcomes the problem of high side-lobes [8].

Various geometries have been proposed and used to solve the problem of direction-of-arrival estimation. They include uniform circular array (UCA), uniform linear array (ULA) [9], uniform rectangular array (URA) [10], among others. Uniform hexagonal arrays (UHA) and uniform circular array (UCA) geometries are compared using particle swarm optimization technique. The arrays consist of 18 elements which are uniformly arranged with a radius of $r = \frac{9}{2\pi}\lambda$. UHA geometries accord moderately deeper nulls, greater gain, and a lesser overall size, as compared to UCA geometries [11]. Hexagonal arrays have been used for direction finding using a Unitary ESPRIT technique. The technique is expanded to 2-dimension direction finding with the uniform rectangular array. Unitary ESPRIT gives a computationally systematic direction finding technique for hexagonal arrays [7].

A precision direction finding of a plane wave from a far-field source to receiving sensors can improve wireless communication system capacity [12]. The minimum variance of any unbiased estimator is referred to as the Cramér-Rao bound (CRB). Determining the Cramér-Rao bound is extremely useful since it provides a benchmark for comparing the achievement of any unbiased estimator and helps to eliminate impossible estimators [2]. CRB is used as a standard measure in the assessment of the accuracy of an estimator since its estimate can be evaluated for various practice settings and it is an important tool for practical design [13]. CRB can be used to forecast how a specific plan choice

impacts the photometric and astrometric achievement of the designed instrument [14]. Cramér-Rao bound is used to describe the achievement of direction finding in antennas arrays. Recently, CRB equations for uniform circular arrays with directive antennas were derived [6]. However, this study did not investigate the CRB of the uniform hexagonal array with isotropic sensors.

Various methods have been used to solve the DOA estimation problem in different dimensions. They include Maximum likelihood [10], Multiple Signal Classification (MUSIC), Estimation of Signal Parameters via Rotational Invariance Techniques (ESPRIT) [15], among others. MUSIC and ESPRIT are Eigen-decomposition algorithms, that determines the DOA estimation by decomposing the covariance matrix to get eigenvectors and eigenvalues [16]. Maximum Likelihood method maximizes the log-likelihood function in order to determine the direction of arrival [17]. Maximum likelihood estimation is too compound to be executed in 2-dimension estimation problems [7].

UCA is able to provide 360 degrees of coverage in the azimuth plane [18]. ULA has perfect orientation and forms a small main-lobe in a certain direction [19]. However, the geometries mentioned above have not solved the problem of high-side lobes [8]. To the best of author's knowledge, there is scanty use of the uniform hexagonal array for the direction of arrival estimation using the CRB. In addition, this paper provides a clear derivation of CRB for direction finding using the uniform hexagonal array and compares the CRB of the uniform hexagonal array with that of the uniform circular array.

The paper is organized as follows: In section 2, the array manifold vector for uniform hexagonal array and the uniform circular array is presented. In Section 3, the description of a detailed CRB implementation is given. The main steps of its derivation are outlined. Results and discussion are presented in Section 4. Graphical representation is presented in section 5. In Section 6 normalized sensitivity analysis is presented. Finally, the conclusion is highlighted in Section 7.

2 Array Manifold Vector for Uniform Hexagonal Array and Uniform Circular Array

2.1 Uniform Circular Array

A circle of radius R centered at the Cartesian origin and lying on the xy-plane is considered. M number of isotropic sensors are uniformly distributed on the circumference of the circle, with equal inter-sensor spacing as shown in Figure 2.1. In Figure 2.1, the central point of the array is at the origin of a Cartesian coordinate system. The sensor located at the positive x-axis is denoted as S_1 while the remaining sensors are uniformly arranged counterclockwise on the circumference of the circle. A complex-valued incident signal from a far-field source impinge on the sensors at an azimuth angle of ϕ, measured counterclockwise from the positive x-axis and a polar angle θ, measured clockwise from the positive z-axis. The location of the m^{th} sensor for $m = 1, 2, \cdots, M$ is given by

$$\mathbf{p}_m = \left[R\cos\left(\tfrac{2\pi(m-1)}{M}\right),\ R\sin\left(\tfrac{2\pi(m-1)}{M}\right),\ 0\right]^T. \tag{2.1}$$

The time delay is given by [20]

$$\tau_m = \frac{\mathbf{v}(\theta,\phi)^T\mathbf{p}_m}{c}. \tag{2.2}$$

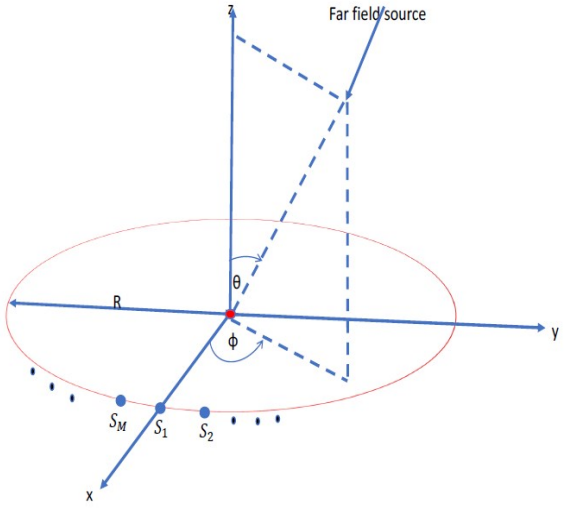

Fig. 1. A Sketch of Uniform Circular Array

In the above, c is the velocity of light and $\mathbf{p}_m$ is the location of the m^{th} sensor. Using (2.1) in (2.2), the array manifold vector for uniform circular array is [20]

$$\mathbf{a}_{\text{UCA}}(\theta,\phi) = \begin{bmatrix} \exp\left\{i\frac{2\pi R}{\lambda}\sin(\theta)\cos(\phi)\right\} \\ \exp\left\{i\frac{2\pi R}{\lambda}\sin(\theta)\cos\left(\phi-\frac{2\pi}{M}\right)\right\} \\ \exp\left\{i\frac{2\pi R}{\lambda}\sin(\theta)\cos\left(\phi-\frac{4\pi}{M}\right)\right\} \\ \vdots \\ \exp\left\{i\frac{2\pi R}{\lambda}\sin(\theta)\cos\left(\phi-\frac{2\pi(M-1)}{M}\right)\right\} \end{bmatrix}. \tag{2.3}$$

2.2 Uniform Hexagonal Array

A hexagon of edge length R centered at the Cartesian origin and lying on the xy-plane is considered. M number of isotropic sensors are uniformly distributed on the circumference of the hexagon, with equal inter-sensor spacing. See Figure 2.2. A complex-valued incident signal from a far-field source impinge on an array of sensors at an azimuth angle ϕ, measured counterclockwise from the positive x-axis and a polar angle θ, measured clockwise from the positive z-axis. The general distance from the center of an equilateral triangle to any sensor is given by

$$x_k = \frac{R}{2}\sqrt{3+\left[\frac{2k-1}{n-1}\right]^2} \tag{2.4}$$

where n is even number of sensors in an equilateral triangle, $M = 6, 18, 30\cdots$ and $k = 1, 2, \cdots, \frac{n}{2}$.

The location of the m^{th} sensor is given by

$$\mathbf{p}_m = \left[x_k\cos\left(\tfrac{2\pi(m-1)}{M}\right),\ x_k\sin\left(\tfrac{2\pi(m-1)}{M}\right)\ ,\ 0\right]^T. \tag{2.5}$$

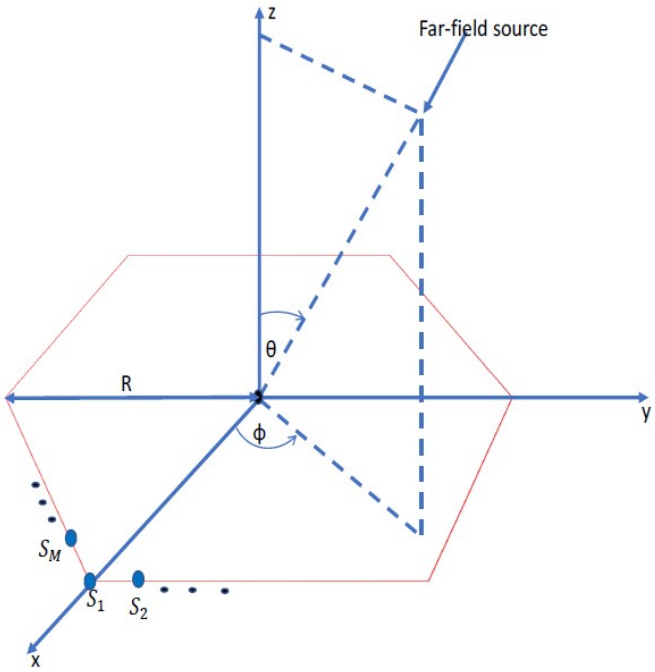

Fig. 2. A Sketch of Uniform Hexagonal Array

Using (2.5) in (2.2), the array manifold vector for the UHA is

$$\mathbf{a}_{\text{UHA}}(\theta,\phi) = \begin{bmatrix} \exp\left\{i\frac{2\pi x_k}{\lambda}\sin(\theta)\ \cos(\phi)\right\} \\ \exp\left\{i\frac{2\pi x_k}{\lambda}\sin(\theta)\ \cos\left(\phi-\frac{2\pi}{M}\right)\right\} \\ \exp\left\{i\frac{2\pi x_k}{\lambda}\sin(\theta)\ \cos\left(\phi-\frac{4\pi}{M}\right)\right\} \\ \vdots \\ \exp\left\{i\frac{2\pi x_k}{\lambda}\sin(\theta)\ \cos\left(\phi-\frac{2\pi(M-1)}{M}\right)\right\} \end{bmatrix}. \tag{2.6}$$

3 Derivation Of The Cramér-Rao Bound

The signal collected by all the sensors at time t can be expressed as

$$\mathbf{y}(t) \quad = \quad \mathbf{a}(\theta,\phi)\underbrace{\sigma_s \exp\{2\pi f t+\varphi\}}_{s(t)} + \mathbf{n}(t), \tag{3.1}$$

where $\mathbf{a}(\theta,\phi)$ is the array manifold vector, $\mathbf{y}(t)$ is the observed data vector, $\mathbf{n}(t)$ is the noise and it is assumed to be zero-mean additive white Gaussian and $s(t)$ is the signal. If there exists T number of discrete-time samples, the observed data vector is represented as [21]

$$\tilde{\mathbf{y}} \quad = \quad \mathbf{s}\otimes\mathbf{a}(\theta,\phi)+\tilde{\mathbf{n}}. \tag{3.2}$$

Direction of arrival estimation aims to estimate the polar arrival angle θ and the azimuth angle ϕ, based on the observations $\tilde{\mathbf{y}}$.

We need to determine the Fisher information matrix (FIM) whose (t,r)-th entry is [22],

$$\begin{aligned}[\mathbf{F}(\boldsymbol{\xi})]_{t,r} &= 2\mathrm{Re}\left\{\left[\frac{\partial \boldsymbol{\mu}}{\partial \xi_t}\right]^H \boldsymbol{\Gamma}^{-1}\left[\frac{\partial \boldsymbol{\mu}}{\partial \xi_r}\right]\right\} \\ &\quad +\mathrm{Tr}\left\{\boldsymbol{\Gamma}^{-1}\frac{\partial \boldsymbol{\Gamma}}{\partial \xi_t}\boldsymbol{\Gamma}^{-1}\frac{\partial \boldsymbol{\Gamma}}{\partial \xi_r}\right\}, \end{aligned} \tag{3.3}$$

where ξ_j is the j-th entry of $\boldsymbol{\xi} = [\theta, \phi]$.

In (3.3), $\mathrm{Re}\{\cdot\}$ and $\mathrm{Tr}\{\cdot\}$ denote the real part and the trace of the identity inside the curly brackets respectively, the superscript H denotes conjugate transposition. For the this given statistical data model,

$$\begin{aligned}\boldsymbol{\mu} &= E[\tilde{\mathbf{y}}] = \mathbf{s} \otimes \mathbf{a}(\theta, \phi), \\ \boldsymbol{\Gamma} &= \sigma_n^2 \mathbf{I}_{TM \times TM}, \end{aligned} \tag{3.4}$$

where $E[\tilde{\mathbf{y}}]$ represents the statistical expectation of $\tilde{\mathbf{y}}$, M denotes the number of sensors, and $\mathbf{I}_{TM\times TM}$ symbolizes an identity matrix of size TM. $\boldsymbol{\Gamma}$ is independent of θ and ϕ, as shown in (3.4), thus the second term of (3.3) is equal to zero.

3.1 Cramér-Rao Bound for the Uniform Circular Array

Differentiating $\boldsymbol{\mu}$ partially with respect to θ we obtain

$$\begin{aligned}&\frac{\partial \boldsymbol{\mu}}{\partial \theta} \\ &= \mathbf{s} \otimes \left\{ \begin{bmatrix} i\frac{2\pi R}{\lambda}\cos(\theta)\cos(\phi) \\ i\frac{2\pi R}{\lambda}\cos(\theta)\cos\left(\phi - \frac{2\pi}{M}\right) \\ i\frac{2\pi R}{\lambda}\cos(\theta)\cos\left(\phi - \frac{4\pi}{M}\right) \\ \vdots \\ i\frac{2\pi R}{\lambda}\cos(\theta)\cos\left(\phi - \frac{2\pi(M-1)}{M}\right) \end{bmatrix} \odot \mathbf{a}(\theta, \phi) \right\}, \end{aligned} \tag{3.5}$$

Differentiating $\boldsymbol{\mu}$ partially with respect to ϕ we obtain

$$\begin{aligned}&\frac{\partial \boldsymbol{\mu}}{\partial \phi} \\ &= \mathbf{s} \otimes \left\{ \begin{bmatrix} -i\frac{2\pi R}{\lambda}\sin(\theta)\sin(\phi) \\ -i\frac{2\pi R}{\lambda}\sin(\theta)\sin\left(\phi - \frac{2\pi}{M}\right) \\ -i\frac{2\pi R}{\lambda}\sin(\theta)\sin\left(\phi - \frac{4\pi}{M}\right) \\ \vdots \\ -i\frac{2\pi R}{\lambda}\sin(\theta)\sin\left(\phi - \frac{2\pi(M-1)}{M}\right) \end{bmatrix} \odot \mathbf{a}(\theta, \phi) \right\}, \end{aligned} \tag{3.6}$$

where $\odot$ denotes the Hadamard product and $\otimes$ denotes the Kronecker product.

Substituting equation (3.5) into equation (3.3), we have

$$F_{\theta,\theta} = 4\pi^2 MT \left(\frac{R}{\lambda}\right)^2 \left(\frac{\sigma_s}{\sigma_n}\right)^2 \cos^2(\theta), \tag{3.7}$$

Substituting equation (3.6) into equation (3.3), we have

$$F_{\phi,\phi} = 4\pi^2 MT \left(\frac{R}{\lambda}\right)^2 \left(\frac{\sigma_s}{\sigma_n}\right)^2 \sin^2(\theta), \tag{3.8}$$

Substituting equations (3.6) and (3.5) into (3.3), we have

$$F_{\theta,\phi} \quad = \quad 0. \tag{3.9}$$

The inverse of Fisher information matrix gives the Cramér-rao bound of θ and ϕ [22]:

$$\begin{bmatrix} \mathrm{CRB}(\theta) & * \\ * & \mathrm{CRB}(\phi) \end{bmatrix} \quad = \quad \begin{bmatrix} F_{\theta,\theta} & F_{\theta,\phi} \\ F_{\phi,\theta} & F_{\phi,\phi} \end{bmatrix}^{-1}, \tag{3.10}$$

where $*$ are terms not of interest.

From (3.10):

$$\mathrm{CRB}_{\mathrm{UCA}}(\theta) \quad = \quad \frac{1}{4\pi^2}\frac{1}{MT}\left(\frac{\lambda}{R}\right)^2\left(\frac{\sigma_n}{\sigma_s}\right)^2 \sec^2(\theta), \tag{3.11}$$

$$\mathrm{CRB}_{\mathrm{UCA}}(\phi) \quad = \quad \frac{1}{4\pi^2}\frac{1}{MT}\left(\frac{\lambda}{R}\right)^2\left(\frac{\sigma_n}{\sigma_s}\right)^2 \csc^2(\theta), \tag{3.12}$$

where T is the total number of time signals and M is the total number of the sensors.

3.2 Cramér-Rao Bound for the Uniform Hexagonal Array

Differentiating $\boldsymbol{\mu}$ partially with respect to θ we obtain

$$\begin{aligned} &\frac{\partial \boldsymbol{\mu}}{\partial \theta} \\ &= \mathbf{s} \otimes \left\{ \begin{bmatrix} i\frac{2\pi x_k}{\lambda}\cos(\theta)\cos(\phi) \\ i\frac{2\pi x_k}{\lambda}\cos(\theta)\cos(\phi - \frac{2\pi}{M}) \\ i\frac{2\pi x_k}{\lambda}\cos(\theta)\cos(\phi - \frac{4\pi}{M}) \\ \vdots \\ i\frac{2\pi x_k}{\lambda}\cos(\theta)\cos\left(\phi - \frac{2\pi(M-1)}{M}\right) \end{bmatrix} \odot \mathbf{a}(\theta,\phi) \right\}, \end{aligned} \tag{3.13}$$

Differentiating $\boldsymbol{\mu}$ partially with respect to ϕ we obtain

$$\begin{aligned} &\frac{\partial \boldsymbol{\mu}}{\partial \phi} \\ &= \mathbf{s} \otimes \left\{ \begin{bmatrix} -i\frac{2\pi x_k}{\lambda}\sin(\theta)\sin(\phi) \\ -i\frac{2\pi x_k}{\lambda}\sin(\theta)\sin(\phi - \frac{2\pi}{M}) \\ -i\frac{2\pi x_k}{\lambda}\sin(\theta)\sin(\phi - \frac{4\pi}{M}) \\ \vdots \\ -i\frac{2\pi x_k}{\lambda}\sin(\theta)\sin\left(\phi - \frac{2\pi(M-1)}{M}\right) \end{bmatrix} \odot \mathbf{a}(\theta,\phi) \right\}. \end{aligned} \tag{3.14}$$

Substituting equation (3.13) into (3.3), we have

$$F_{\theta,\theta} \quad = \quad 4MT\pi^2\left(\frac{x_k}{\lambda}\right)^2\left(\frac{\sigma_s}{\sigma_n}\right)^2\cos^2(\theta). \tag{3.15}$$

Substituting equation (3.14) into (3.3), we have

$$F_{\phi,\phi} \quad = \quad 4MT\pi^2\left(\frac{x_k}{\lambda}\right)^2\left(\frac{\sigma_s}{\sigma_n}\right)^2\sin^2(\theta). \tag{3.16}$$

Substituting equation (3.13) and equation (3.14) into (3.3), we have

$$F_{\theta,\phi} \quad = \quad 0.$$

Using equation (3.15) in (3.10) Cramér-rao bound of θ is found to be:

$$\mathrm{CRB}_{\mathrm{UHA}}(\theta) \quad = \quad \frac{1}{4\pi^2}\frac{1}{MT}\left(\frac{\lambda}{x_k}\right)^2\left(\frac{\sigma_n}{\sigma_s}\right)^2 \sec^2(\theta). \tag{3.17}$$

Using equation (3.16) in (3.10) Cramér-rao bound of ϕ is found to be:

$$\mathrm{CRB}_{\mathrm{UHA}}(\phi) \quad = \quad \frac{1}{4\pi^2}\frac{1}{MT}\left(\frac{\lambda}{x_k}\right)^2\left(\frac{\sigma_n}{\sigma_s}\right)^2 \csc^2(\theta). \tag{3.18}$$

4 Results Analysis and Discussion

From (3.17)-(3.18) and (3.11)-(3.12) the ratio of Cramér-rao bound of uniform hexagonal array to that of uniform circular array is;

$$\begin{aligned}\frac{\mathrm{CRB}_{\mathrm{UHA}}(\theta)}{\mathrm{CRB}_{\mathrm{UCA}}(\theta)} \;=\; \frac{\mathrm{CRB}_{\mathrm{UHA}}(\phi)}{\mathrm{CRB}_{\mathrm{UCA}}(\phi)} \quad &= \quad \left(\frac{2}{\sqrt{3+[\frac{2k-1}{n-1}]^2}}\right)^2 \\ &:= \quad \frac{\mathrm{CRB}_{\mathrm{UHA}}}{\mathrm{CRB}_{\mathrm{UCA}}}.\end{aligned} \tag{4.1}$$

where $\mathrm{CRB}_{\mathrm{UHA}}$ and $\mathrm{CRB}_{\mathrm{UCA}}$ denote the CRBs for the UHA and UCA, respectively.

We consider all possible scenarios of equation (4.1) as analyzed in the following cases.

When the ratio $\frac{\mathrm{CRB}_{\mathrm{UHA}}}{\mathrm{CRB}_{\mathrm{UCA}}}$ is greater than one we have

4.1 Case 1: $\left(\frac{2}{\sqrt{3+[\frac{2k-1}{n-1}]^2}}\right)^2 > 1$

$$\sqrt{3+\left[\frac{2k-1}{n-1}\right]^2} < 2 \quad \Leftrightarrow \quad k < \frac{n}{2}. \tag{4.2}$$

Equation (4.2) holds for

$$\begin{aligned} n = 4;\ k = 1; M = 18 \\ n = 6;\ k = 1, 2; M = 30 \\ n = 8;\ k = 1, 2, 3; M = 42 \\ \vdots \end{aligned}$$

When the above conditions hold, the $\mathrm{CRB}_{\mathrm{UHA}}$ are higher as compared to $\mathrm{CRB}_{\mathrm{UCA}}$, implying that UCA has better performance as compared to UHA.

Consider condition $n = 6;\ k = 1, 2;\ M = 30$:

$$\mathrm{CRB}_{\mathrm{UHA}}(\theta) = \frac{1}{4\pi^2}\frac{1}{30T}\left(\frac{1.14707\lambda}{R}\right)^2\left(\frac{\sigma_n}{\sigma_s}\right)^2 \sec^2(\theta), \tag{4.3}$$

and

$$\mathrm{CRB}_{\mathrm{UCA}}(\theta) \quad = \quad \frac{1}{4\pi^2}\frac{1}{30T}\left(\frac{\lambda}{R}\right)^2\left(\frac{\sigma_n}{\sigma_s}\right)^2\sec^2(\theta). \tag{4.4}$$

When the ratio $\frac{\mathrm{CRB}_{\mathrm{UHA}}}{\mathrm{CRB}_{\mathrm{UCA}}}$ is less than one we have

4.2 Case 2: $\left(\frac{2}{\sqrt{3+[\frac{2k-1}{n-1}]^2}}\right)^2 < 1$

When $\left(\frac{2}{\sqrt{3+[\frac{2k-1}{n-1}]^2}}\right)^2 < 1$, we have that

$$\sqrt{3+\left[\frac{2k-1}{n-1}\right]^2} > 2 \quad \Leftrightarrow \quad k > \frac{n}{2}. \tag{4.5}$$

This case is not a possible scenario since the general distance derived in equation (2.4) holds for k not exceeding $\frac{n}{2}$. Thus it is established that under no circumstance will $\mathrm{CRB}_{\mathrm{UHA}}$ be lower than $\mathrm{CRB}_{\mathrm{UCA}}$. When the ratio $\frac{\mathrm{CRB}_{\mathrm{UHA}}}{\mathrm{CRB}_{\mathrm{UCA}}}$ is equal to one we have

4.3 Case 3: $\left(\frac{2}{\sqrt{3+[\frac{2k-1}{n-1}]^2}}\right)^2 = 1$

$$\sqrt{3+[\frac{2k-1}{n-1}]^2} = 2 \quad \Leftrightarrow \quad k = \frac{n}{2}. \tag{4.6}$$

Equation (4.6) holds for

$$\begin{gathered} n=2;\ k=1;\ M=6 \\ n=4;\ k=2;\ M=18 \\ n=6;\ k=3;\ M=30 \\ \vdots \end{gathered}$$

When the above conditions holds, UHA and UCA have the same performance.

Consider condition $n=2; k=1; M=6$:

$$\mathrm{CRB}_{\mathrm{UHA}}(\theta) = \frac{1}{4\pi^2}\frac{1}{6T}\left(\frac{\lambda}{R}\right)^2\left(\frac{\sigma_n}{\sigma_s}\right)^2\sec^2(\theta), \tag{4.7}$$

and

$$\mathrm{CRB}_{\mathrm{UCA}}(\theta) \quad = \quad \frac{1}{4\pi^2}\frac{1}{6T}\left(\frac{\lambda}{R}\right)^2\left(\frac{\sigma_n}{\sigma_s}\right)^2\sec^2(\theta). \tag{4.8}$$

In the above, $n = 2, 4, 6, \cdots, N$ denotes the total number of the sensors on one of the equilateral triangle of the uniform hexagonal array and M is the total number of the sensors.

5 Graphical Representation

Figure 5 to 5 present numerical simulation of the ratio developed in Section4. Figure 5 shows that increase in n and k, results into increased ratio $\frac{\text{CRB}_{\text{UHA}}}{\text{CRB}_{\text{UCA}}}$. Figure 5 indicates that when $k < \frac{n}{2}$ increases, it results to an decrease in the ratio, implying that uniform circular array performs better than uniform hexagonal array. When $k = \frac{n}{2}$, the ratio is equal to one but at point $20, 30, 40$ there are some depression this is as a result of bifurcation as n crosses some values. The values of the ratio at those points still equals one as shown in Figure 5, thus the geometries have the same performance. Finally, the case when $k > \frac{n}{2}$ is not a possible scenario since the ratio is converging to zero, as indicated in Figure 5. Mathematica software was used to perform the following simulations.

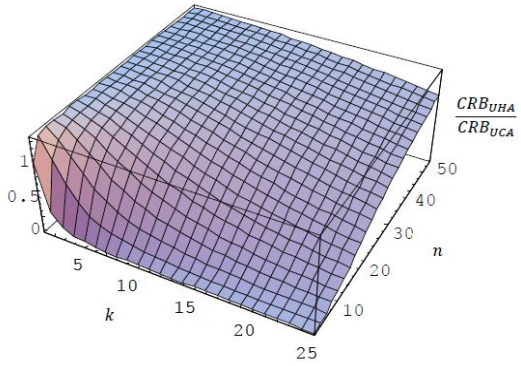

Fig. 3. The figure shows how the ratio $\frac{\text{CRB}_{\text{UHA}}}{\text{CRB}_{\text{UCA}}}$ changes as n and k changes

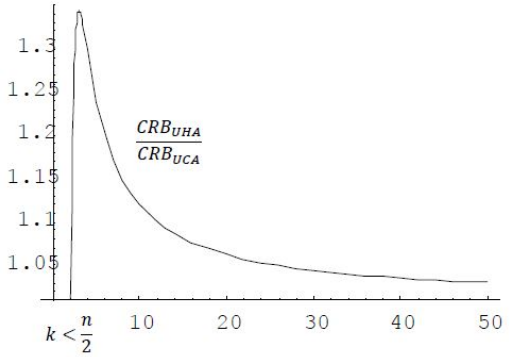

Fig. 4. The figure shows how the ratio $\frac{\text{CRB}_{\text{UHA}}}{\text{CRB}_{\text{UCA}}}$ changes as $k < \frac{n}{2}$ varies.

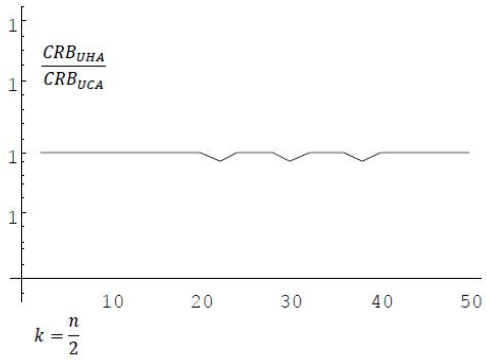

Fig. 5. The figure shows how the ratio $\frac{\mathrm{CRB}_{\mathrm{UHA}}}{\mathrm{CRB}_{\mathrm{UCA}}}$ changes as $k=\frac{n}{2}$ varies

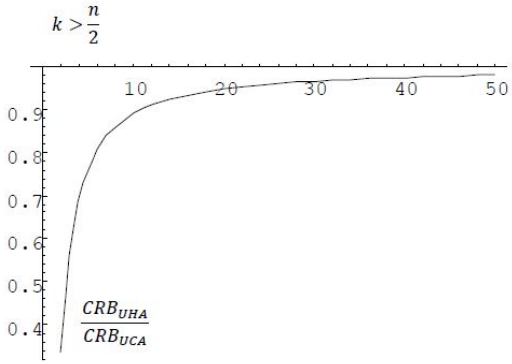

Fig. 6. The figure shows how the ratio $\frac{\mathrm{CRB}_{\mathrm{UHA}}}{\mathrm{CRB}_{\mathrm{UCA}}}$ changes as $k>\frac{n}{2}$ varies

6 Normalized Sensitivity Analysis

Sensitive analysis is an algorithm that is used to determine how self-reliant variable values will influence a particular reliant variable under certain presumption. It helps to examine how sensitive the output is, by the changes in one input while holding the other input constant. Let

$$\frac{\mathrm{CRB}_{\mathrm{UHA}}}{\mathrm{CRB}_{\mathrm{UCA}}}=\frac{4}{3+[\frac{2k-1}{n-1}]^2} \quad = \quad \frac{4(n-1)^2}{3(n-1)^2+(2k-1)^2}. \tag{6.1}$$

The normalized sensitivity analysis of a parameter ω in $f(\omega)$ is given by $S=\frac{\partial f}{\partial \omega}\frac{\omega}{f}$.

We can normalize about some point n and k:

$$\begin{aligned} S_n^1 &= \frac{\partial R}{\partial n}\frac{n}{R} \\ &= \frac{2(1-2k)^2 n}{(n-1)\{4+4(k-1)\}k+3(n-2)n}, \end{aligned} \tag{6.2}$$

$$\begin{aligned} S_k^1 &= \frac{\partial R}{\partial k}\frac{k}{R} \\ &= -\frac{4k(2k-1)}{(2k-1)^2+3(n-1)^2}. \end{aligned} \tag{6.3}$$

The normalized sensitivity of equation (6.2) shows that the ratio increases with increase in n since S_n^1 is always positive for $n \geq 2$ and $k \geq 1$, while equation (6.3) shows that the ratio decreases with increase in k since S_k^1 is always negative for $n \geq 2$ and $k \geq 1$.

7 Conclusion

This paper appears to be first in the open literature to investigate Cramér-Rao bound of the direction-of-arrival estimation using UHA. The key findings are: The Cramér-Rao bound of the uniform hexagonal array decreases with an increase in the number of sensors, therefore, UHA can be used in direction-of-arrival estimation when the number of sensors increases. The comparison between hexagonal and circular arrays shows that hexagonal array geometry give slightly higher Cramér-Rao bound by approximately

$$\frac{2}{\sqrt{3+[\frac{2k-1}{n-1}]^2}} \tag{7.1}$$

with respect to circular arrays.

Acknowledgement

A brief acknowledgement section may be given after the conclusion section just before the references. The acknowledgments of people who provided assistance in manuscript preparation, funding for research, etc. should be listed in this section. All sources of funding should be declared as an acknowledgement. Authors should declare the role of funding agency, if any, in the study design, collection, analysis and interpretation of data; in the writing of the manuscript. If the study sponsors had no such involvement, the authors should so state.

Competing Interests

Declaration of competing interest should be placed here. All authors must disclose any financial and personal relationships with other people or organizations that could inappropriately influence (bias) their work. Examples of potential conflicts of interest include employment, consultancies, honoraria, paid expert testimony, patent applications/registrations, and grants or other funding. If no such declaration has been made by the authors, SDI reserves to assume and write this sentence: Authors have declared that no competing interests exist.

References

[1] Gupta L, Singh RP. Direction of arrival estimation. International Journal of Advanced Engineering Technology. Sept; 2010.

[2] Kay SM. Fundamental of statistical signal processing: Estimation theory. Upper Saddle River, New Jersey: Prentice Hall; 1993.

[3] Ihedrane MA, Seddik BR. Direction of arrival estimation using MUSIC, ESPRIT and maximum-likelihood algorithms for antenna arrays. Walailak Journal of Science and Technology (WJST). 2015;13(6):491-502.

[4] Hong JG, Ahn WH, Seo BS. Compensation of mutual coupling in an antenna array for direction of arrival estimation. 2013 15th International conference on Advanced Communications Technology. 2013;599-603.

[5] Devendra M, Manjunathachari K. Literature survey on high resolution direction of arrival (DOA) algorithm. International Advanced Research Journal in Science, Engineering and Technology. 2015;2.

[6] Jackson BJ, Rajan S, Liao BJ, Wang S. Direction of arrival estimation using directive antennas in uniform circular arrays. IEEE Transactions on Antennas and propagation. 2015;2:736-747.

[7] Tian Z, Van Trees HL. Do a estimation with hexagonal arrays. In Proceeding of the 1998 IEEE International Conference on Acoustic, Speech and Signal processing, ICASSP'98. 1998;4:2053-2056.

[8] Montaser AM, Mahmoud KR, Abdel-Rahman B, Elmikati HA. Circular, hexagonal and octagonal array geometries for smart antenna system using hybrid CFO-HC algorithm. Journal of Engineering Sciences, Assiut University. 2012;40(6):1715-1732.

[9] Bhuiya SN, Islam F, Matin MA. Analysis of direction of arrival techniques using uniform linear array. International Journal of Computer Theory and Engineering. 2012;4(6).

[10] Wu H, Hou C, Chen H, Liu W, Wang Q. Direction finding and mutual coupling estimation for uniform rectangular arrays. Signal Processing. 2015;0165-1684.

[11] Mahmoud KR, El-Adawy M, Ibrahem SM, Bansal R, Zainud-Deen SH. A comparison between circular and hexagonal array geometries for smart antenna systems using particle swarm optimization aligorithm. Progress In Electromagnetics Research. 2007;72:75-90.

[12] Oluwole AS, Srivastava VM. Smart antenna for wireless communication systems using spatial signal processing. Journal of Communications. 2017;12: 6.

[13] Chao J, Ward ES, Ober RJ. Fisher information theory for parameter estimation in single molecule microscopy. 2016;33(7):B36-B57.

[14] Mendez RA, Silva JF, Orostica R, Lobos R. Analysis of the Cramér-Rao bound in the joint estimation of astrometry and photometry. Publication of Astronomical Society of the Pacific 2016. 2014;942:798.

[15] Ihedranel MA, Bri S. Direction of arrival estimation using music, esprit and maximum-likelihood algorithms for antenna arrays. Walailak J Sci and Tech. 2016;13(6):491-502.

[16] Kim JT, Kim ST, Lee KW. Ambiguity analysis method for the calibrated array manifold; 2013.

[17] Li M, Lu Y, B He. Array signal processing for maximum likelihood direction-of-Arrival estimation. Li et al., J Electr Electron Syst. 2013;3(10.4172):2332-0796.1000117.

[18] Vesa A. Direction-of-Arrival estimation in case of uniform sensor array using the MUSIC algorithm. Transactions on electronics and communication. 56:40.

[19] Sun B. MUSIC based on uniform circular array and its direction-finding efficiency. Inte. J. Sign. Proc. Syst. 2013;1:273-277.

[20] Van Trees HL. Optimum array processing: Part IV of detection, estimation and modulation theory. John Wiley and Sons; 2004.

[21] Kitavi DM, Tan H, Wong KT. A regular tetrahedral array whose constituent sensors fail randomly. A lower bound for direction-of-arrival estimation. Loughborough Antennas and Propagation Conference (LAPC); 2016.

[22] Kitavi DM, Wong KT, Hung CC. An L-shaped array with nonorthogonal axes its Cramér-Rao bound for direction finding. IEEE Transactions on Aerospace and Electronic Systems. 2018;54(1):486-492.

Peer-review history:
The peer review history for this paper can be accessed here (Please copy paste the total link in your browser address bar)
http://www.sdiarticle3.com/review-history/48163